Bioconjugate Chemistry

Communication

pubs.acs.org/bc

An Amphiphilic Perylene Imido Diester for Selective Cellular Imaging

Timm Heek,[†] Jörg Nikolaus,[‡] Roland Schwarzer,[‡] Carlo Fasting,[†] Pia Welker,[§] Kai Licha,[§] Andreas Herrmann,*[,‡] and Rainer Haag*[,†]

[†]Institut für Chemie und Biochemie, Freie Universität Berlin, Takustraße 3, 14195 Berlin, Germany

[‡]Institut für Biologie/Molekulare Biophysik, Humboldt Universität zu Berlin, Invalidenstraße 42, 10115 Berlin, Germany

[§]mivenion GmbH, Robert-Koch-Platz 4, 10115 Berlin, Germany

Supporting Information

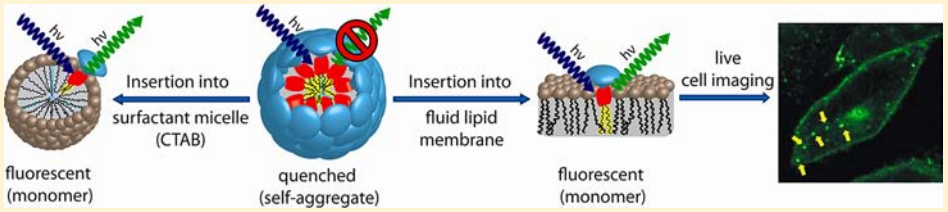

ABSTRACT: A new amphiphilic membrane marker based on a water-soluble dendritic polyglycerol perylene imido dialkylester has been designed, synthesized, and its optical properties characterized. In water it forms fluorescently quenched micellar self-aggregates, but when incorporated into a lipophilic environment, it monomerizes, and the highly fluorescent properties of the perylene core are recovered. These properties make it an ideal candidate for the imaging of artificial and cellular membranes as demonstrated by biophysical studies.

INTRODUCTION

A key challenge in cellular imaging is the ability to stain different cell compartments with high specificity and persistence in order to understand and track biological processes in detail. Especially the plasma membrane is of tremendous interest due to the fact that it plays a major role in cellular uptake, cell trafficking, and signal transduction. Therefore, amphiphilic dyes, such as commercially available dialkylcarbocyanines, are among the most used dyes in the staining and characterization of artificial and biological membranes.[1−6] However, their stabilities, especially upon extended irradiation, are limited.

Derivatives of perylene-3,4,9,10-tetracarboxylic acid bisanhydride (PBA) have been extensively employed in a broad range of different fields from their use as color pigments in industrial paints and lacquers up to applications in organic electronics, light harvesting arrays, and the construction of supramolecular architectures.[7−17] In general, perylene-based dyes possess a set of favorable properties like high extinction coefficients, high quantum yields, and high chemical and photophysical stability. However, solubility is always a problem when dealing with such polyaromatic structures, as they tend to form insoluble aggregates via strong $\pi-\pi$ interactions, which is even more pronounced in an aqueous environment.[18] Nevertheless, due to their excellent photophysical properties, there has been increasing interest in the production of highly water-soluble perylene derivatives in order to apply them in the field of cellular imaging.[19−26]

However, besides one amphiphilic, ionic perylenemonoimide, which has been used in the characterization of lipid rafts in living Jurkat cells, most of the reported water-soluble perylene derivatives show a rather unspecific uptake into the cytoplasma of living cells.[24] Usually, upon insertion into the exoplasmic leaflet of the plasma membrane, perylene derivatives rapidly move to the cytoplasmic leaflet from which they redistribute to intracellular membranes.[27] Thus, these lipid probes have several limitations. For example, they are not faithful labels for tracking endocytic pathway of plasma membrane lipids, as they can bypass this pathway. In contrast, analogues of typical phospholipids, for example, phosphatidylcholine, which is one major lipid component in the exoplasmic leaflet of the plasma membrane of mammalian cells, cannot rapidly move to the cytoplasmic leaflet and redistribute to intracellular membranes.

To circumvent these limitations, we designed an amphiphilic perylene derivative which has a stable localization at the exoplasmic leaflet of the plasma membrane, is water-soluble to be applicable without the addition of any organic cosolvent or additive in biological systems, and offers the possibility of modification of the perylene core for further spectral tuning. To introduce high water solubility to the perylene core, we decided to use polyglycerol (PG) dendrons, as they have been shown to be highly efficient in solubilizing perylene tetracarboxylic acid bisimides (PBI) in aqueous media.[26,28] In contrast to ionic hydrophilic groups, this should guarantee that the properties of the probe are independent of pH and ionic strength, which is often high in biological buffer systems. In addition, it minimizes artifacts which may occur through unspecific ionic interactions.

Received: November 14, 2012
Revised: December 19, 2012
Published: January 7, 2013

   dx.doi.org/10.1021/bc3005655 | *Bioconjugate Chem.* 2013, 24, 153−158

For high membrane specificity, we decided to use a perylene imido diester (PIDE) bearing two alkyl chains as membrane anchoring groups. The length of the aliphatic chains was chosen so that the overall length of the hydrophobic part is around 2 nm, which matches the thickness of one lipid bilayer leaflet. To test its versatility as an efficient membrane marker, we investigated the photophysical behavior via UV/vis and fluorescence spectroscopy in different solvents and applied it to the imaging of artificial membranes as well as of living cells.

RESULTS AND DISCUSSION

Synthesis of the PG-Dendronized Membrane Marker. The synthesis of the amphiphilic membrane marker follows an efficient route over four steps (Scheme 1). Although other

Scheme 1. Design and Synthesis of the Amphiphilic Perylene Dye [G3]-PIDE-C_{10} for Imaging of Biological Membranes[a]

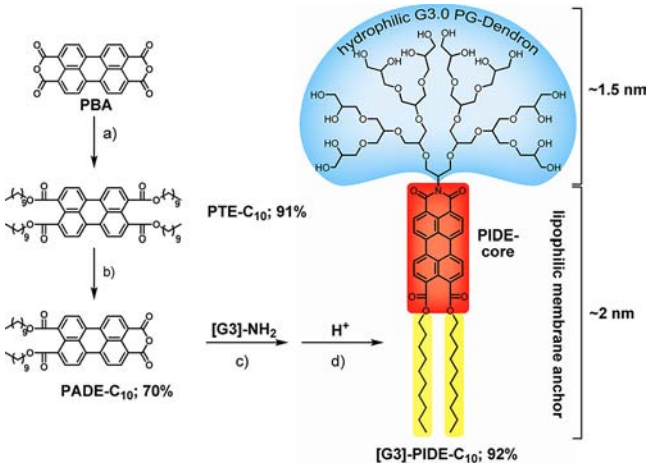

[a]Reaction Conditions: (a) i. KOH, H_2O, 70 °C, 20 min, ii. TOAB, KI, RT, 20 min, iii. 1-bromodecane, reflux, 18 h; (b) PTSA·H_2O, toluene/*n*-dodecane 1:5, 95 °C, 2 h; (c) [G3]-NH_2, imidazole, 140 °C, 4 h; (d) TFA, DMSO/H_2O 1:3, 50 °C, 24 h.

synthetic pathways toward asymmetric PIDEs are known, this route is the most economical with respect to the used amine.[29,30] The perylene anhydride diester (PADE-C_{10}) was synthesized according to literature procedures, which involved the preparation of the corresponding perylene tetracarboxylic acid tetraalkyester (PTE-C_{10}) under phase transfer conditions[31] and a subsequent partial hydrolysis.[32] In the last step, an acetal-protected, core-aminated PG dendron of the third generation [G3][33,34] was condensed to the monoanhydride in an imidazole melt at 140 °C. A subsequent cleavage of the acetal protecting groups under acidic conditions with TFA in a DMSO/water mixture led to the final product [G3]-PIDE-C_{10} in good yield.

Photophysical Properties. [G3]-PIDE-C_{10} shows a strong absorption (Figure 1a) in the visible region between 400 and 560 nm related to the electronic S_0–S_1 transition that makes it suitable for one-photon fluorescence microscopy measurements (using 488 nm Ar-laser excitation line). It is readily soluble in a broad variety of polar organic solvents and even in bare water (>10^{-2} M). For a complete list of tested solvents refer to Table S1 in the Supporting Information. The extinction coefficient varies only slightly within the tested solvents between 42 000 and 46 600 cm^{-1} at the absorption maximum with the exception of water (*vide infra*). The fluorescence (Figure 1b) resembles a mirror image of the absorption with moderate stokes shifts between 21 to 35 nm and high quantum yields up to Φ = 0.98 in dioxane. The fluorescence lifetimes were measured and showed monoexponential decays with lifetimes varying between 4.0 and 4.6 ns similar to lifetimes for related PBIs or PTEs.[35] Due to the amphiphilicity in water, drastic differences in the optical properties were observed. The main peak of the absorption is hypsochromically shifted from between 500 and 510 nm in organic solvents to 483 nm in water accompanied by a decrease of the extinction coefficient to 24 900 cm^{-1} and a loss of the vibronic fine structure. Furthermore, there is an increase in the absorbance between 540 and 600 nm. This behavior can be interpreted based on exciton coupling theory in terms of the formation of H-type aggregates with a rotational displacement between adjacent dye molecules and has been observed for structurally related aggregated PBIs in organic solvents.[36−38] The fluorescence properties also change dramatically. The fine structure is completely lost, and only a weak, unstructured fluorescence signal with a maximum at 621 nm and a quantum yield of Φ = 0.01 is observed. This can be attributed to the formation of an excimer-type excited state and has been observed for other aggregated PIDEs.[39,40] Further investigations via dynamic light scattering and transmission electron microscopy support the aggregate formation and clearly indicate spherical micelles with a diameter of 9 ± 1 nm and a rather narrow size distribution (Supporting Information, Figure S1).

To see whether these aggregates could be broken up in an aqueous surrounding a titration with varying amounts of the cationic surfactant cetyltrimethylammoniumbromid (CTAB) was performed. The absorption and fluorescence spectra for a CTAB treated PIDE-solution can be seen in Figure 1c,d. Above a surfactant concentration of 1 mM, which corresponds to the critical micelle concentration (cmc) of CTAB,[41−43] the well-resolved absorption and fluorescence signals corresponding to the monomeric species were reestablished with a quantum yield of Φ = 0.72. This behavior is extremely useful because this probe is nearly nonfluorescent in bare water, and if efficiently incorporated into a lipophilic environment, fluorescence recovery close to the theoretical maximum is possible. In a biological sample this would lead to a strong contrast from the actually stained material to the surrounding aqueous medium (Figure 2). Similar concepts of increasing the signal-to-noise ratio of target-specific probes through H-Dimer formation have been reported, e.g., for Xanthene-based dyes.[44,45]

The photostability of the probe was tested in comparison to other commercial available membrane markers like C6-NDB-PC, fluorescein-C18, and DiO.[46−48] Therefore, a small amount of a 10^{-6} M solution of the corresponding dye in DMSO was irradiated with a 400 mW Ar-laser for 1 h and the remaining intensity measured. As can be seen in Figure 3a, G3-PIDE-C_{10} shows the lowest bleaching with 52% of the intensity remaining. Especially when comparing this with the DiO carbocyanine (26% intensity remaining), which is one of the most photostable green fluorescent membrane markers, this proves the high photostability of the new marker.

Artifical Membrane Staining. After these basic photophysical studies, we investigated the incorporation of [G3]-PIDE-C_{10} into artificial lipid bilayers. Therefore, small unilamellar vesicles (SUVs) prepared from dioleoylphosphatidylcholine (DOPC) were added stepwise to a 1 μM solution of [G3]-PIDE-C_{10}. Similar to the solution treated with surfactant, there was an increase of the monomer fluorescence with a maximum at 534 nm after each addition of vesicles, which

dx.doi.org/10.1021/bc3005655 | *Bioconjugate Chem.* 2013, 24, 153−158

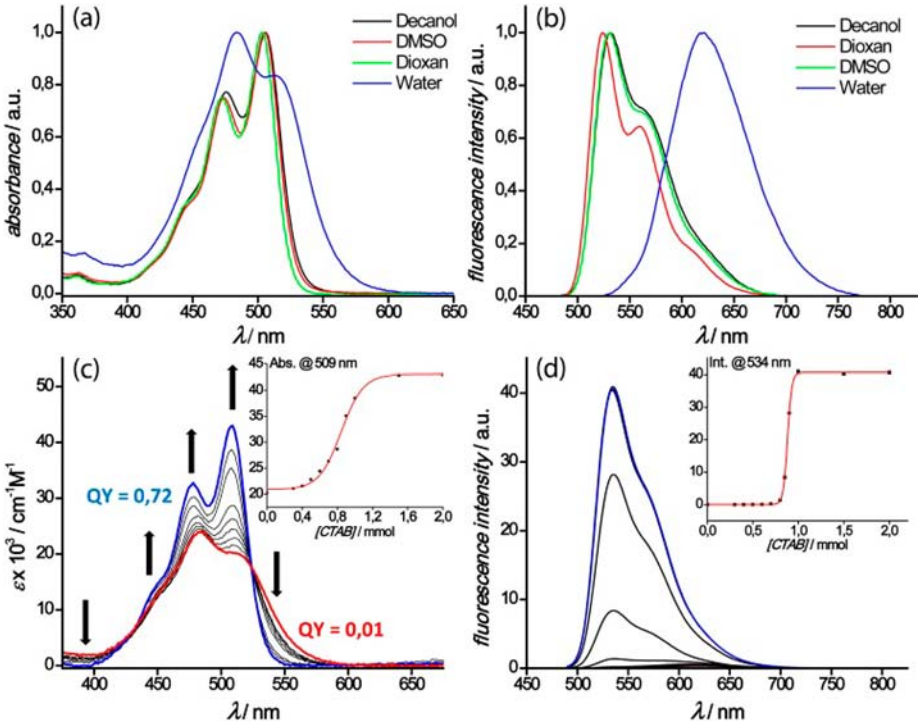

Figure 1. Normalized absorption (a) and fluorescence (b) spectra of [G3]-PIDE-C_{10} in various solvents (1 μM, 20 °C). (c) Effect of CTAB on the absorption spectrum of [G3]-PIDE-C_{10} in water (1 μM). The red line represents the absorption spectrum in water without the addition of surfactant. The black lines represent an increasing amount of CTAB. The blue line represents the final spectrum at the highest surfactant concentration (20 mM). The arrows indicate spectral changes upon addition. The inset shows the plot of absorbance at 509 nm versus CTAB concentration. (d) Fluorescence spectra (λ_{ex} = 474−484 nm) corresponding to the absorption spectra in panel (c). The inset shows the plot of fluorescence intensity at 534 nm versus CTAB concentration.

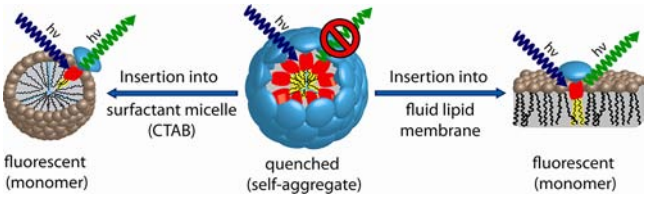

Figure 2. Schematic function of the self-quenched amphiphilic dye [G3]-PIDE-C_{10} upon monomerization within different environments.

shows that the dye was efficiently incorporated into the membranes (Figure 3b). As the partitioning of a membrane marker into different lipid domains is of great interest, we further prepared vesicles of different lipid compositions to reflect the different phases.[49] Therefore, in addition to DOPC vesicles which represent the liquid disordered (L_d) phase, vesicles with dipalmitoylphosphatidylcholine (DPPC) for the gel phase (L_{gel}) and a mixture of DPPC with cholesterol (7:3) for the liquid ordered (L_o) phase were prepared and the influence of the lipid packing on the fluorescence behavior was examined. In all cases, a monomeric fluorescence signal could be detected with the intensity decreasing in the order of DOPC > DPPC > DPPC/cholesterol (Supporting Information, Figure S2) which shows that the dye was incorporated into the membrane of all different compositions with a high preference to the liquid disordered phase. To visualize this selectivity in more detail, giant unilamellar vesicles (GUVs) were prepared with a raft-mix consisting of DOPC, stearoylsphingomyelin (SSM), and cholesterol in a molar ratio of 1:1:1, yielding vesicles with coexisting L_d/L_o domains large enough to be visualized via fluorescence microscopy. As can be seen in Figure 3c, there is a strong preference of [G3]-PIDE-C_{10} for one phase. Using Rh-DOPE as a costaining lipidic dye, which is known to partition preferentially to the L_d domains, this domain is attributed to be the L_d-domain.[50,51] If fluorescence intensities are taken as a measure for the partitioning, the ratio of the incorporation from [G3]-PIDE-C_{10} between L_d and L_o is 95% to 5%, rendering it a useful fluid phase marker for disordered domains.

Cellular Uptake Studies. Having shown that the dye is easily incorporated into artificial membranes, the uptake into living cells was investigated. To this end, different cell lines were probed: Chinese ovary hamster (CHO), baby hamster kidney (BHK) cells, and the human lung cancer cell line A549. As a prerequisite for application in cell imaging, the probe should be nontoxic. Therefore, cell toxicity was measured via the MTT-cell activity assay and via CASY. After incubation for 48 h with varying concentrations up to 10^{-5} M, no cytotoxic effects were observed showing that the probe is completely nontoxic (Supporting Information, Figure S3). Accordingly, cells were incubated with a 10^{-5} M dye solution and the uptake over time followed via confocal laser scanning microscopy (CLSM). As depicted for CHO cells in Figure 4 (other cells see Supporting Information, Figure S4), after 25 min [G3]-PIDE-C_{10} is strongly accumulated in the plasma membrane, small vesicular structures, and in the Golgi apparatus near the cell nucleus.

This distribution pattern indicates that cellular uptake of the dye occurs via endocytic routes after being incorporated into the plasma membrane. This is further supported by two facts. First, in short-term incubation experiments up to 10 min, the dye is essentially located only in the plasma membrane (Figure

dx.doi.org/10.1021/bc3005655 | Bioconjugate Chem. 2013, 24, 153−158

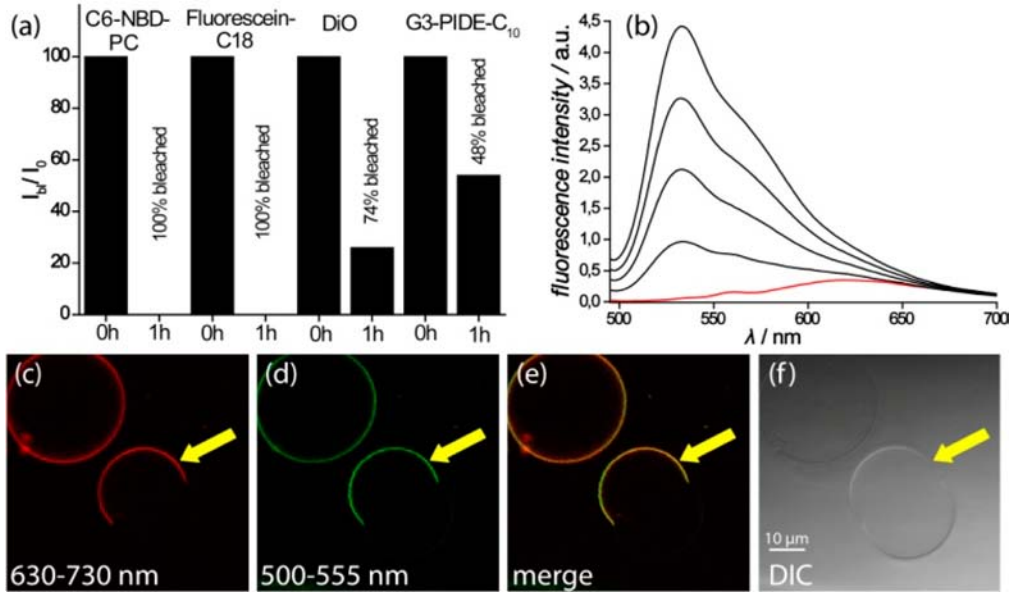

Figure 3. (a) Bleaching experiments of 1 μM solutions of different membrane markers in DMSO before and after 1 h argon laser irradiation. (b) Fluorescence increase of [G3]-PIDE-C_{10} upon successive addition of small unilamellar lipid vesicles (red line representing pure dye solution). (c–f) Confocal fluorescence microscopy images of GUVs (Raft-mix DOPC/SSM/Chol molar ratio 1:1:1) incubated with 1 μM of [G3]-PIDE-C_{10} for 10 min and counterstained with N–Rh-DOPE. (a) N–Rh-DOPE, (b) [G3]-PIDE-C_{10}, (c) overlay of both signals, and (d) DIC image. Yellow arrows point to the L_d domains.

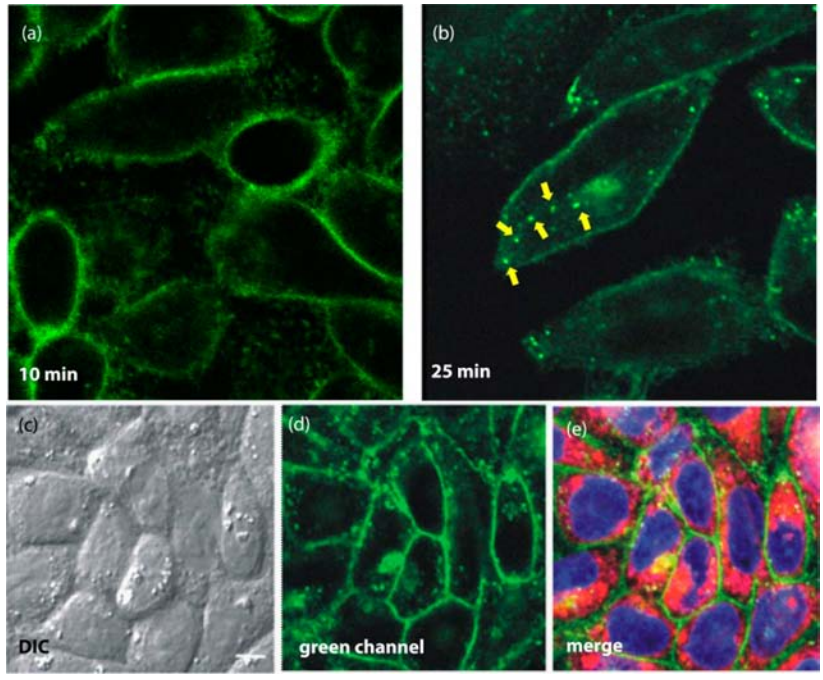

Figure 4. Confocal microscopy images of CHO cells incubated with [G3]-PIDE-C_{10}. (a) Short time incubation for 10 min showing exclusive labeling of the plasma membrane and (b) incubation for 25 min showing endocytic uptake of the dye. The yellow arrows point to vesicles most likely trafficking toward the Golgi apparatus. (c–e) Costaining experiment with BODIPY-TR methyl ester (red) for intracellular membranes and DAPI (blue) for cell nucleus. The yellow color indicates colocalization from BODIPY with [G3]-PIDE-C_{10} at the Golgi apparatus.

4a). Second, inhibition of endocytic uptake by incubation of cells at low temperature (4 °C) or by an inhibitor of endocytic transport showed a strongly decreased dye uptake as revealed by microscopy and FACS analysis (Supporting Information, Figures S6–S8). Furthermore, we can exclude that the staining from the intracellular structures arises from a passive diffusion of [G3]-PIDE-C_{10} through the plasma membrane, as the costaining with BODIPY TR methyl ester, a passive entering dye which efficiently stains membranes of intracellular organelles such as ER, Golgi apparatus, and mitochondria, shows no colocalization with [G3]-PIDE-C_{10} with the exception of the Golgi.[52] Longer incubation times did not change this distribution pattern significantly, and the same intracellular labeling pattern was observed for the other cell lines (Supporting Information, Figures S4–S7).

dx.doi.org/10.1021/bc3005655 | *Bioconjugate Chem.* 2013, 24, 153–158

CONCLUSION

In summary, we have synthesized and characterized a new water-soluble membrane marker based on an amphiphilic dendritic polyglycerol perylene imido dialkylester which forms fluorescence quenched aggregates in water but becomes highly green fluorescent when incorporated into a lipophilic environment, such as biological membranes. We could show that it can be easily used as fluid phase marker for disordered domains in artificial membranes and that it is efficiently taken up into living cells following endocytic pathways. Due to its high quantum yield, high photophysical stability, and easy modifiability on the dendron side, it is an ideal platform to anchor and track polyglycerol bound bioactive compounds in artificial or cellular membranes.

ASSOCIATED CONTENT

Supporting Information

Experimental details about the synthesis and the experimental setup used. This material is available free of charge via the Internet at http://pubs.acs.org.

AUTHOR INFORMATION

Corresponding Author

*E-mail: andreas.herrmann@rz.hu-berlin.de; haag@chemie.fu-berlin.de.

Notes

The authors declare no competing financial interest.

ACKNOWLEDGMENTS

The authors thank the Deutsche Forschungsgemeinschaft (DFG) for financial support via the SFB 765 and acknowledge the focus area Nanoscale of the Freie Universität Berlin for the enabling structure (www.nanoscale.fu-berlin.de).

REFERENCES

(1) Schlessinger, J., Axelrod, D., Koppel, D., Webb, W., and Elson, E. (1977) Lateral transport of a lipid probe and labeled proteins on a cell membrane. *Science 195*, 307−309.

(2) Struck, D. K., and Pagano, R. E. (1980) Insertion of fluorescent phospholipids into the plasma membrane of a mammalian cell. *J. Biol. Chem. 255*, 5404−5410.

(3) Honig, M. G., and Hume, R. I. (1989) DiI and DiO: versatile fluorescent dyes for neuronal labeling and pathway tracing. *Trends Neurosci. 12*, 333−341.

(4) Kahya, N., Scherfeld, D., Bacia, K., Poolman, B., and Schwille, P. (2003) Probing lipid mobility of raft-exhibiting model membranes by fluorescence correlation spectroscopy. *J. Biol. Chem. 278*, 28109−28115.

(5) Heberle, F. A., Buboltz, J. T., Stringer, D., and Feigenson, G. W. (2005) Fluorescence methods to detect phase boundaries in lipid bilayer mixtures. *Biochim. Biophys. Acta 1746*, 186−192.

(6) Thomas, J. L., Holowka, D., Baird, B., and Webb, W. W. (1994) Large-scale co-aggregation of fluorescent lipid probes with cell surface proteins. *J. Cell Biol. 125*, 795−802.

(7) Zollinger, H. (2003) *Color chemistry. Syntheses, properties, and applications of organic dyes and pigments*, 3rd ed., Wiley-VCH, Weinheim.

(8) Herbst, W. (2004) *Industrial organic pigments. Production, properties, applications*, 3rd ed., Wiley-VCH, Weinheim.

(9) Huang, C., Barlow, S., and Marder, S. R. (2011) Perylene-3,4,9,10-tetracarboxylic acid diimides: synthesis, physical properties, and use in organic electronics. *J. Org. Chem. 76*, 2386−2407.

(10) Li, C., and Wonneberger, H. (2012) Perylene imides for organic photovoltaics: yesterday, today, and tomorrow. *Adv. Mater. 24*, 613−636.

(11) Weil, T., Reuther, E., and Müllen, K. (2002) Shape-persistent, fluorescent polyphenylene dyads and a triad for efficient vectorial transduction of excitation energy. *Angew. Chem. 114*, 1980−1984.

(12) Baffreau, J., Ordronneau, L., Leroy-Lhez, S., and Hudhomme, P. (2008) Fullerene C_{60} − perylene-3,4:9,10-bis(dicarboximide) light-harvesting dyads: spacer length and bay-substituent effects on intramolecular singlet and triplet energy transfer. *J. Org. Chem. 73*, 6142−6147.

(13) Kirmaier, C., Song, H.-e., Yang, E., Schwartz, J. K., Hindin, E., Diers, J. R., Loewe, R. S., Tomizaki, K.-y., Chevalier, F., and Ramos, L. (2010) Excited-state photodynamics of perylene-porphyrin dyads. 5. Tuning light-harvesting characteristics via perylene substituents, connection motif, and three-dimensional architecture. *J. Phys. Chem. B 114*, 14249−14264.

(14) Flamigni, L., Ventura, B., You, C.-C., Hippius, C., and Würthner, F. (2007) Photophysical characterization of a light-harvesting tetra naphthalene imide/perylene bisimide array. *J. Phys. Chem. C 111*, 622−630.

(15) Würthner, F. (2004) Perylene bisimide dyes as versatile building blocks for functional supramolecular architectures. *Chem. Commun. 14*, 1564−1579.

(16) Würthner, F. (2006) Bay-substituted perylene bisimides: Twisted fluorophores for supramolecular chemistry. *Pure Appl. Chem. 78*, 2341−2349.

(17) Krieg, E., and Rybtchinski, B. (2011) Noncovalent water-based materials: robust yet adaptive. *Chem.—Eur. J. 17*, 9016−9026.

(18) Chen, Z., Lohr, A., Saha-Möller, C. R., and Würthner, F. (2009) Self-assembled π-stacks of functional dyes in solution: structural and thermodynamic features. *Chem. Soc. Rev. 38*, 564−584.

(19) Gao, B., Li, H., Liu, H., Zhang, L., Bai, Q., and Ba, X. (2011) Water-soluble and fluorescent dendritic perylene bisimides for live-cell imaging. *Chem. Commun. 47*, 3894−3896.

(20) Wang, L., Xu, L., Neoh, K. G., and Kang, E.-T. (2011) Water-soluble highly fluorescent poly[poly(ethylene glycol) methyl ether methacrylate] for cell labeling. *J. Mater. Chem. 21*, 6502−6505.

(21) Weil, T., Abdalla, M. A., Jatzke, C., Hengstler, J., and Müllen, K. (2005) Water-soluble rylene dyes as high-performance colorants for the staining of cells. *Biomacromolecules 6*, 68−79.

(22) Peneva, K., Mihov, G., Nolde, F., Rocha, S., Hotta, J.-i., Braeckmans, K., Hofkens, J., Uji-I, H., Herrmann, A., and Müllen, K. (2008) Water-soluble monofunctional perylene and terrylene dyes: powerful labels for single-enzyme tracking. *Angew. Chem., Int. Ed. 47*, 3372−3375.

(23) Zhao, Y., Zhang, X., Li, D., Liu, D., Jiang, W., Han, C., and Shi, Z. (2009) Water-soluble 3,4:9,10-perylene tetracarboxylic ammonium as a high-performance fluorochrome for living cells staining. *Luminescence 24*, 140−143.

(24) Margineanu, A., Hotta, J.-i., van der Auweraer, M., Ameloot, M., Stefan, A., Beljonne, D., Engelborghs, Y., Herrmann, A., Müllen, K., and de Schryver, F. C. (2007) Visualization of membrane rafts using a perylene monoimide derivativeand fluorescence lifetime imaging. *Biophys. J. 93*, 2877−2891.

(25) Céspedes-Guirao, F. J., Ropero, A. B., Font-Sanchis, E., Nadal, Á., Fernández-Lázaro, F., and Sastre-Santos, Á. (2011) A water-soluble perylene dye functionalised with a 17β-estradiol: a new fluorescent tool for steroid hormones. *Chem. Commun. 47*, 8307−8309.

(26) Yang, S. K., Shi, X., Park, S., Doganay, S., Ha, T., and Zimmerman, S. C. (2011) Monovalent, clickable, uncharged, water-soluble perylenediimide-cored dendrimers for target-specific fluorescent biolabeling. *J. Am. Chem. Soc. 133*, 9964−9967.

(27) Pagano, R. E., Ozato, K., and Ruysschaert, J. M. (1977) Intracellular distribution of lipophilic fluorescent probes in mammalian cells. *Biochim. Biophys. Acta 465* (3), 661−666.

(28) Heek, T., Fasting, C., Rest, C., Zhang, X., Würthner, F., and Haag, R. (2010) Highly fluorescent water-soluble polyglycerol-dendronized perylene bisimide dyes. *Chem. Commun. 46*, 1884−1886.

(29) Kelber, J., Bock, H., Thiebaut, O., Grelet, E., and Langhals, H. (2011) Room temperature columnar liquid crystalline perylene imido-diesters via a homogeneous one-pot imidification-esterification of

perylene 3,4,9,10-tetracarboxylic anhydride. *Eur. J. Org. Chem.*, 707−712.
(30) Yao, P., Yang, X., Xu, X., Lu, Y., Ji, H.-F., and Dai, S. (2011) Morphologies and optical properties of nanostructures self-assembled from asymmetrical, amphiphilic perylene derivatives. *J. Mater. Sci. 46*, 188−195.
(31) Mo, X., Shi, M.-M., Huang, J.-C., Wang, M., and Chen, H.-Z. (2008) Synthesis, aggregation and photoconductive properties of alkoxycarbonyl substituted perylenes. *Dyes Pigm. 76*, 236−242.
(32) Xue, C., Sun, R., Annab, R., Abadi, D., and Jin, S. (2009) Perylene monoanhydride diester: a versatile intermediate for the synthesis of unsymmetrically substituted perylene tetracarboxylic derivatives. *Tetrahedron Lett. 50*, 853−856.
(33) Wyszogrodzka, M., and Haag, R. (2008) A convergent approach to biocompatible polyglycerol "click" dendrons for the synthesis of modular core−shell architectures and their transport behavior. *Chem.—Eur. J. 14*, 9202−9214.
(34) Wyszogrodzka, M., Möws, K., Kamlage, S., Wodzisńka, J., Plietker, B., and Haag, R. (2008) New approaches towards monoamino polyglycerol dendrons and dendritic triblock amphiphiles. *Eur. J. Org. Chem.*, 53−63.
(35) Langhals, H., Karolin, J., and Johansson, L. B.-Å. (1998) Spectroscopic properties of new and convenient standards for measuring fluorescence quantum yields. *J. Chem. Soc., Faraday Trans. 94*, 2919−2922.
(36) Kasha, M., Rawls, H. R., and Ashraf El-Bayoumi, M. (1965) The exciton model in molecular spectroscopy. *Pure Appl. Chem. 11*, 371−392.
(37) Chen, Z., Stepanenko, V., Dehm, V., Prins, P., Siebbeles, L., Seibt, J., Marquetand, P., Engel, V., and Würthner, F. (2007) Photoluminescence and conductivity of self-assembled pi-pi stacks of perylene bisimide dyes. *Chem.—Eur. J. 13*, 436−449.
(38) Würthner, F., Thalaker, C., Diele, S., and Tschierske, C. (2001) Fluorescent J-type aggregates and thermotropic columnar mesophases of perylene bisimide dyes. *Chem.—Eur. J. 7*, 2245−2253.
(39) Bauman, D., Hertmanowski, R., Stefańska, K., and Stolarski, R. (2011) The synthesis of novel perylene-like dyes and their aggregation properties in Langmuir and Langmuir-Blodgett films. *Dyes Pigm. 91*, 474−480.
(40) Yang, L., Shi, M., Wang, M., and Chen, H. (2008) Synthesis, electrochemical, and spectroscopic properties of soluble perylene monoimide diesters. *Tetrahedron 64*, 5404−5409.
(41) Mukerjee, P., and Mysels, K. J. (1970) *Critical Micelle Concentrations of Aqueous Surfactant Solutions*; National Bureau of Standards.
(42) Kalyanasundaram, K., and Thomas, J. K. (1977) Environmental effects on vibronic band intensities in pyrene monomer fluorescence and their application in studies of micellar systems. *J. Am. Chem. Soc. 99*, 2039−2044.
(43) Aguiar, J., Carpena, P., Molina-Bolívar, J., and Carnero Ruiz, C. (2003) On the determination of the critical micelle concentration by the pyrene 1:3 ratio method. *J. Colloid Interface Sci. 258*, 116−122.
(44) Ogawa, M., Kosaka, N., Choyke, P. L., and Kobayashi, H. (2009) H-Type dimer formation of fluorophores: a mechanism for activatable, *in vivo* optical molecular imaging. *ACS Chem. Biol. 4*, 535−546.
(45) Kobayashi, H., and Choyke, P. L. (2011) Target-cancer-cell-specific activatable fluorescence imaging probes: rational design and in vivo applications. *Acc. Chem. Res. 44*, 83−90.
(46) Kachel, K., Asuncion-Punzalan, E., and London, E. (1998) The location of molecules with charged groups in membranes. *Biochim. Biophys. 1374*, 63−76.
(47) Tan, S. S., Hauser, P. C., Wang, K., Fluri, K., Seiler, K., Rusterholz, B., Suter, G., Krüttli, M., Spichiger, U. E., and Simon, W. (1991) Reversible optical sensing membrane for the determination of chloride in serum. *Anal. Chim. Acta 255*, 35−44.
(48) Sleight, R. G., and Pagano, R. E. (1984) Transport of a fluorescent phosphatidylcholine analog from the plasma membrane to the Golgi apparatus. *J. Cell Biol. 99*, 742−751.
(49) Baumgart, T., Hunt, G., Farkas, E. R., Webb, W. W., and Feigenson, G. W. (2007) Fluorescence probe partitioning between Lo/Ld phases in lipid membranes. *Biochim. Biophys. Acta 1768*, 2182−2194.
(50) de Almeida, R. F., Loura, L. M., Fedorov, A., and Prieto, M. (2005) Lipid rafts have different sizes depending on membrane composition: a time-resolved fluorescence resonance energy transfer study. *J. Mol. Biol. 346*, 1109−1120.
(51) Gudethi, M., Mlodzianoski, M., and Hess, S. (2007) Imaging and shape analysis of GUVs as model plasma membranes: effect of *trans* DOPC on membrane properties. *Biophys. J. 93*, 2011−2023.
(52) Cooper, M. S., Szeto, D. P., Sommers-Herivel, G., Topczewski, J., Solnica-Krezel, L., Kang, H.-C., Johnson, I., and Kimelman, D. (2005) Visualizing morphogenesis in transgenic zebrafish embryos using BODIPY TR methyl ester dye as a vital counterstain for GFP. *Dev. Dyn. 232*, 359−368.